Wavewatch-III and Anisotropic Eddy Transport in Climate Models

Baylor Fox-Kemper, Brown University

Qing Li (Brown) & Scott Reckinger (Brown)
both will present at AGU OS14
plus
Adrean Webb (TUMST), Mark Hemer (CSIRO),
Ramsey Harcourt (UW), Tony Craig, & others

NCAR OMWG, 9:30-9:55, 16-17 January 2014
Main Seminar Room, Mesa Lab

S.C. Bates, B. Fox-Kemper, S.R. Jayne, W.G. Large, S. Stevenson, and S.G. Yeager. Mean biases, variability, and trends in air-sea fluxes and SST in the CCSM4. Journal of Climate, 25(22):7781-7801, November 2012.

Significant Air-Sea Heat Flux Errors vs. Data (Large & Yeager 09)

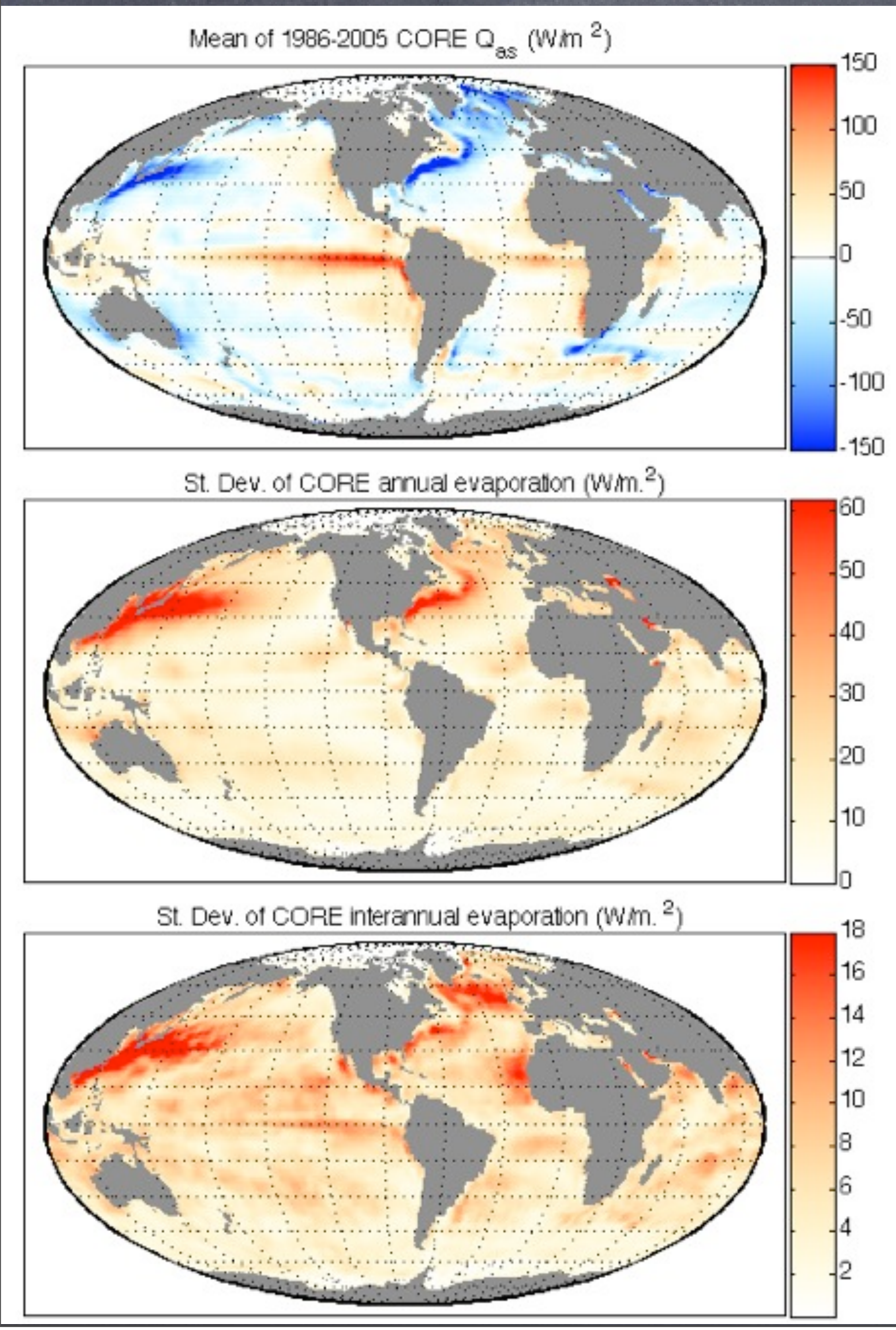

Mean

Annual 9-15mo

Interannual 2-7yr

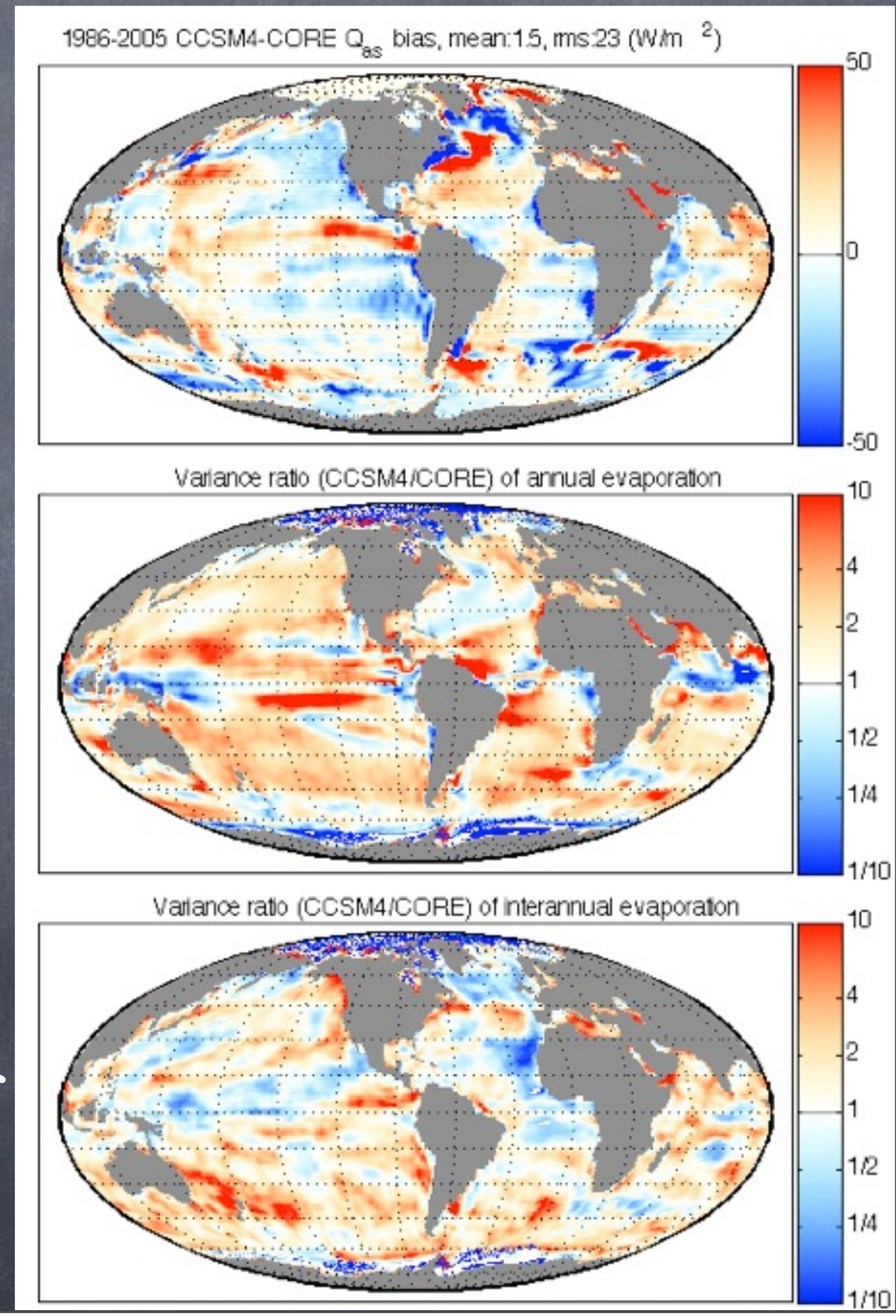

The Character of the Langmuir Scale

- Near-surface
- Langmuir Cells & Langmuir Turb.
- Ro>>1
- Ri<1: Nonhydro
- 10-100m
- 10s to mins
- w, u=O(10cm/s)
- Stokes drift
- Eqns: Craik-Leibovich
- Params: McWilliams & Sullivan, 2000, etc.

Image: Quickbird, Deepwater Horizon Oil Spill

Figure 1a Illustration of Langmuir circulations showing notation used in this review and surface and subsurface motions.

Image: Leibovich, 83

WAVEWATCH III is run as a CESM component, then Large & Yeager (04) Normal Year Ocean Only, 15-month run (Qing Li, new primary)

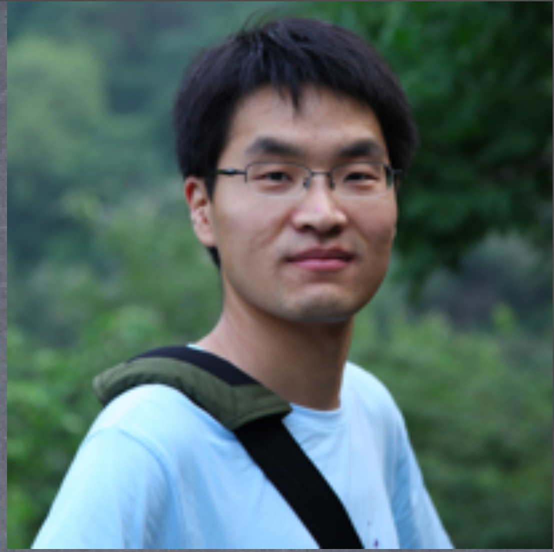

Calculate the Langmuir number $La_t = \sqrt{(u_* / u_s(0))}$ in WW3 and pass it back to POP to update KPP following McWillaims & Sullivan, 2000 (MS2K).

Run a pair of 15-month tests:

Control: Langmuir parameterization off

MS2K: apply an enhancement factor $\epsilon = \sqrt{(1+0.08\, La_t^{-4})}$ to the turbulent velocity magnitude, leaving the coefficient for the non-local flux unchanged currently. I notice that Fan & Griffies used a different factor: $\epsilon = (1+0.2\, La_t^{-1})^2$

Notes:

The interpolation problem between ocean and wave model grids still exists: it generate false values along coastlines when passing the Langmuir number to the ocean. But it is not a big issue here as long as I filter out those extremely small La values: only apply the enhancement factor where La > 0.1

In MS2K I also turn on the Langmuir parameterization that already in the KPP code. It use La to calculate the Langmuir depth and use the Langmuir depth to update the mixed layer depth. I've checked its effect earlier and the mixed layer depth will not change too much when only using this parameterization.

The resolution I use is T31_gx3v7_ww3a

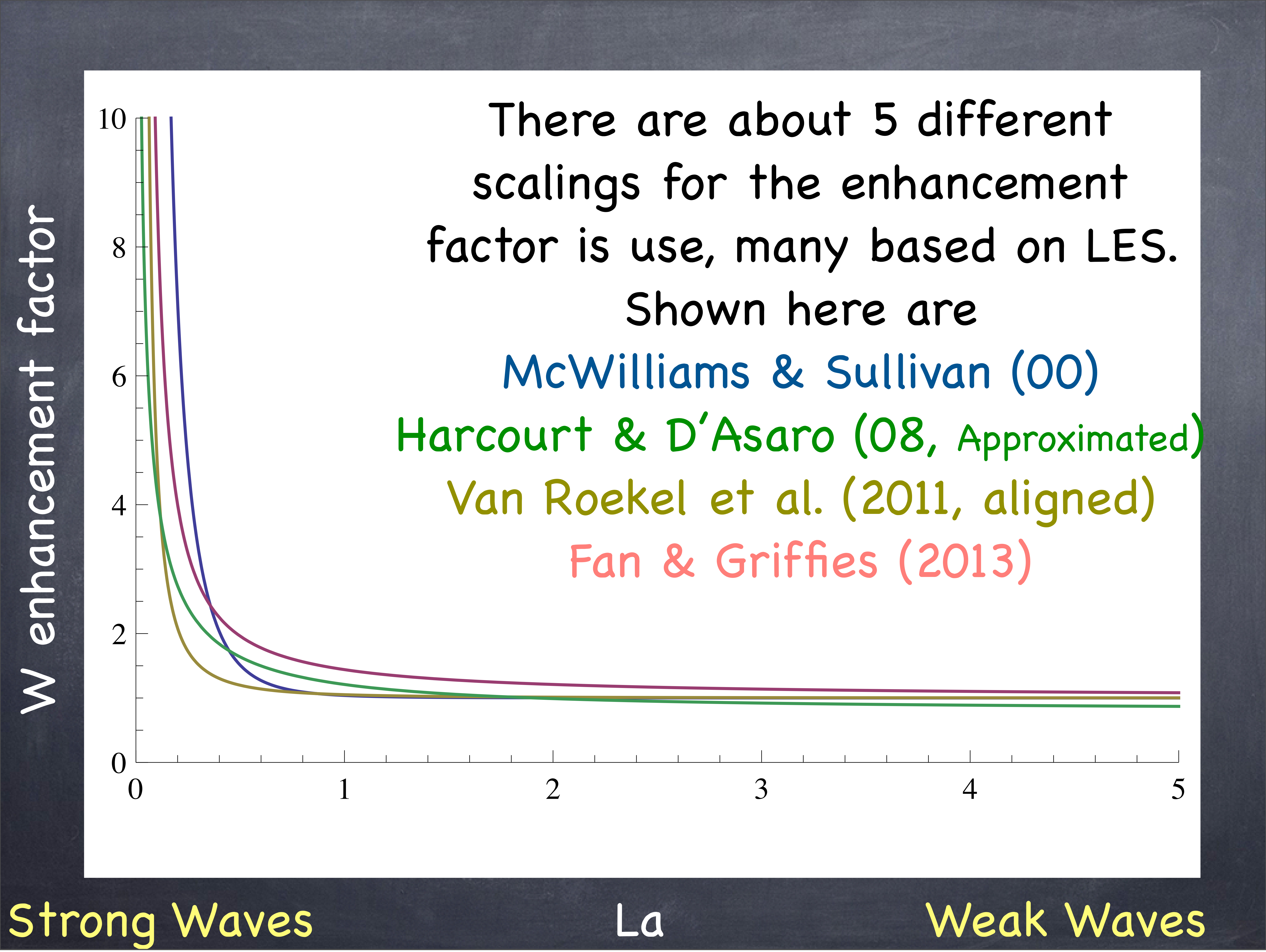

10
8
6
4
2
0
0
1
2
3
4
5
There are about 5 different scalings for the enhancement factor is use, many based on LES.
Shown here are
McWilliams & Sullivan (00)
Harcourt & D'Asaro (08, Approximated)
Van Roekel et al. (2011, aligned)
Fan & Griffies (2013)
W enhancement factor
Strong Waves
La
Weak Waves

Langmuir Number

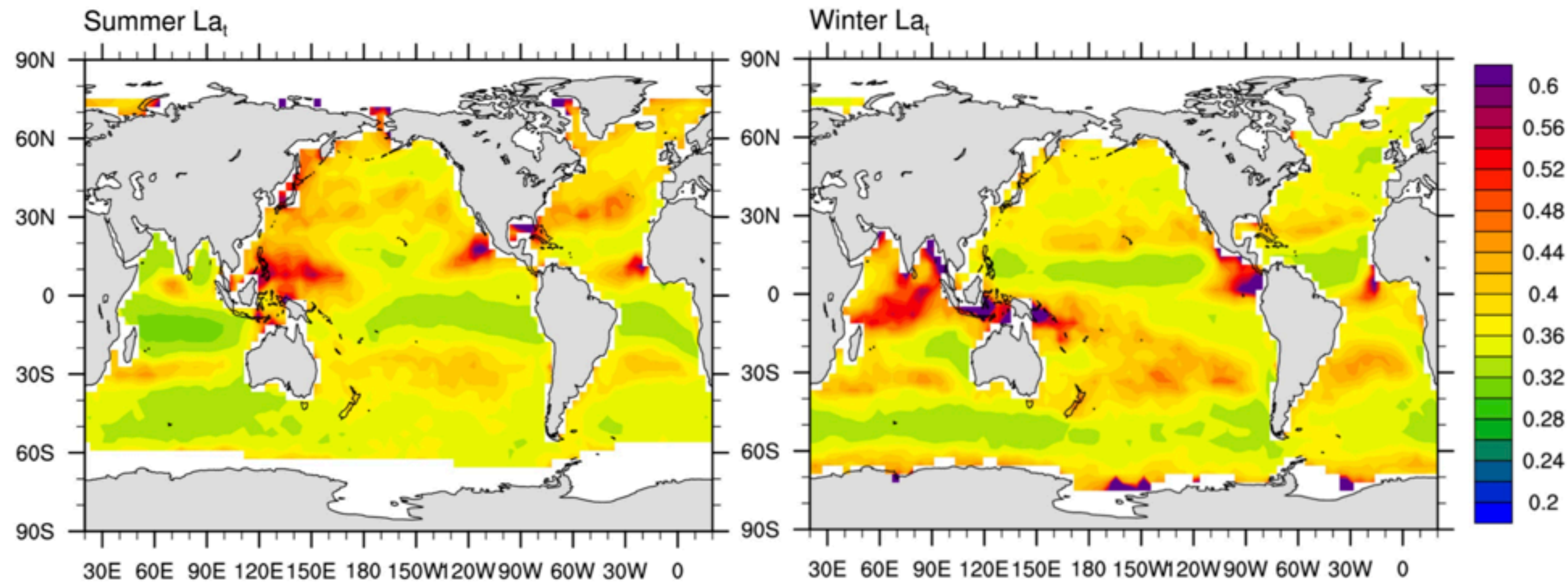

Summer: average over Jul. - Sep. of the first model year

Winter: averaged over Jan. - Mar. of the second model year

WAVEWATCH III is run as a CESM component, then Large & Yeager (04) Normal Year Ocean Only, 15-month run (Qing Li, new primary)

Control

McWilliams-Sullivan, 2000 (MS2K)

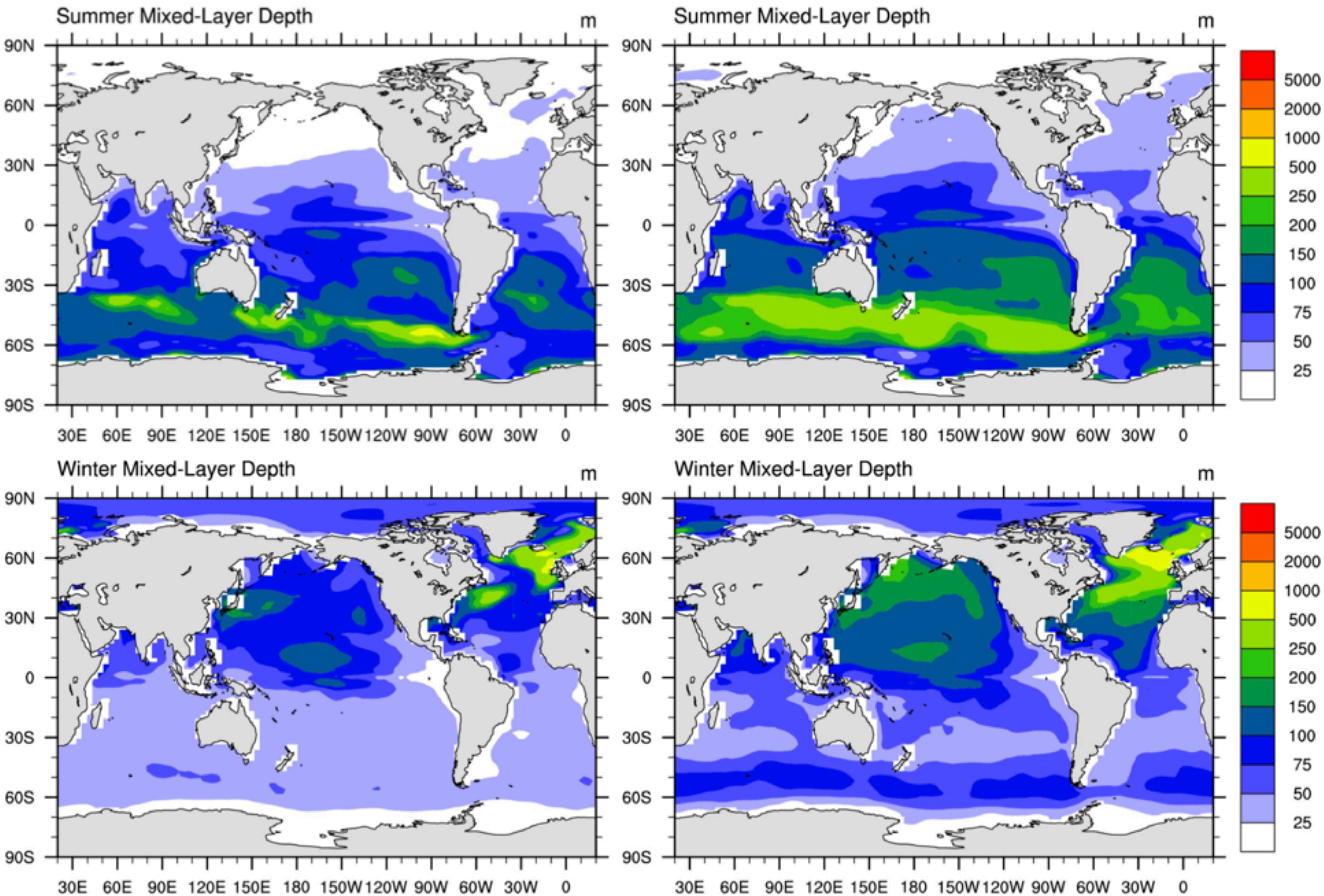

Compare to GFDL CM2M (Fully-Coupled)

Similar results

Fan & Griffies (2013, subm.)

Details differ, both are based on McWilliams & Sullivan (2000)

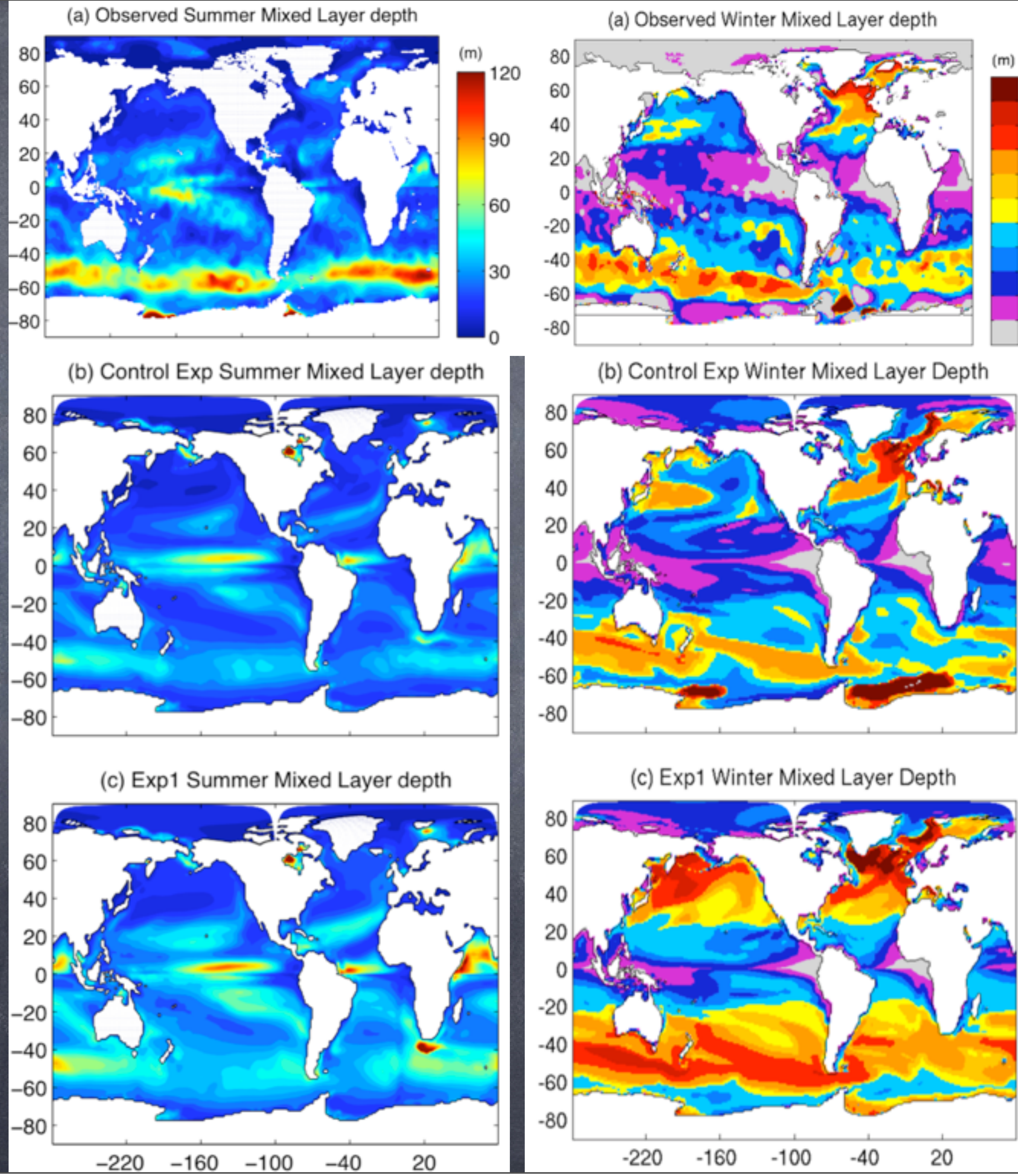

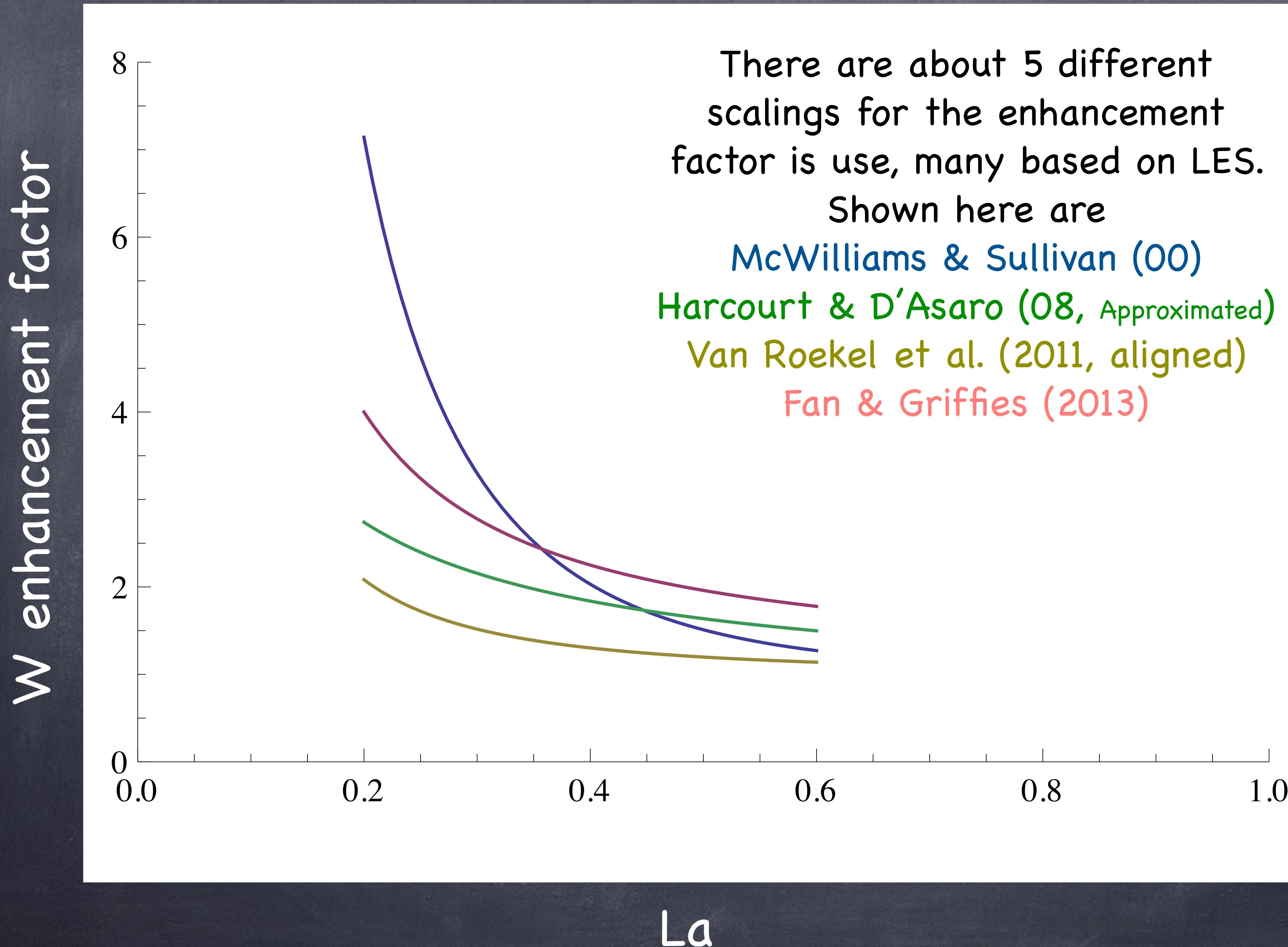
W enhancement factor
8
6
4
2
0
0.0
0.2
0.4
0.6
0.8
1.0
La
There are about 5 different scalings for the enhancement factor is use, many based on LES.
Shown here are
McWilliams & Sullivan (00)
Harcourt & D'Asaro (08, Approximated)
Van Roekel et al. (2011, aligned)
Fan & Griffies (2013)

Offline Calculation using Harcourt (2013) Second-Moment Closure, Argo Initial Conds., and Large & Yeager (04) Normal Year

Less deepening than the CESM/KPP/McW&S & GFDL/KPP/McW&S

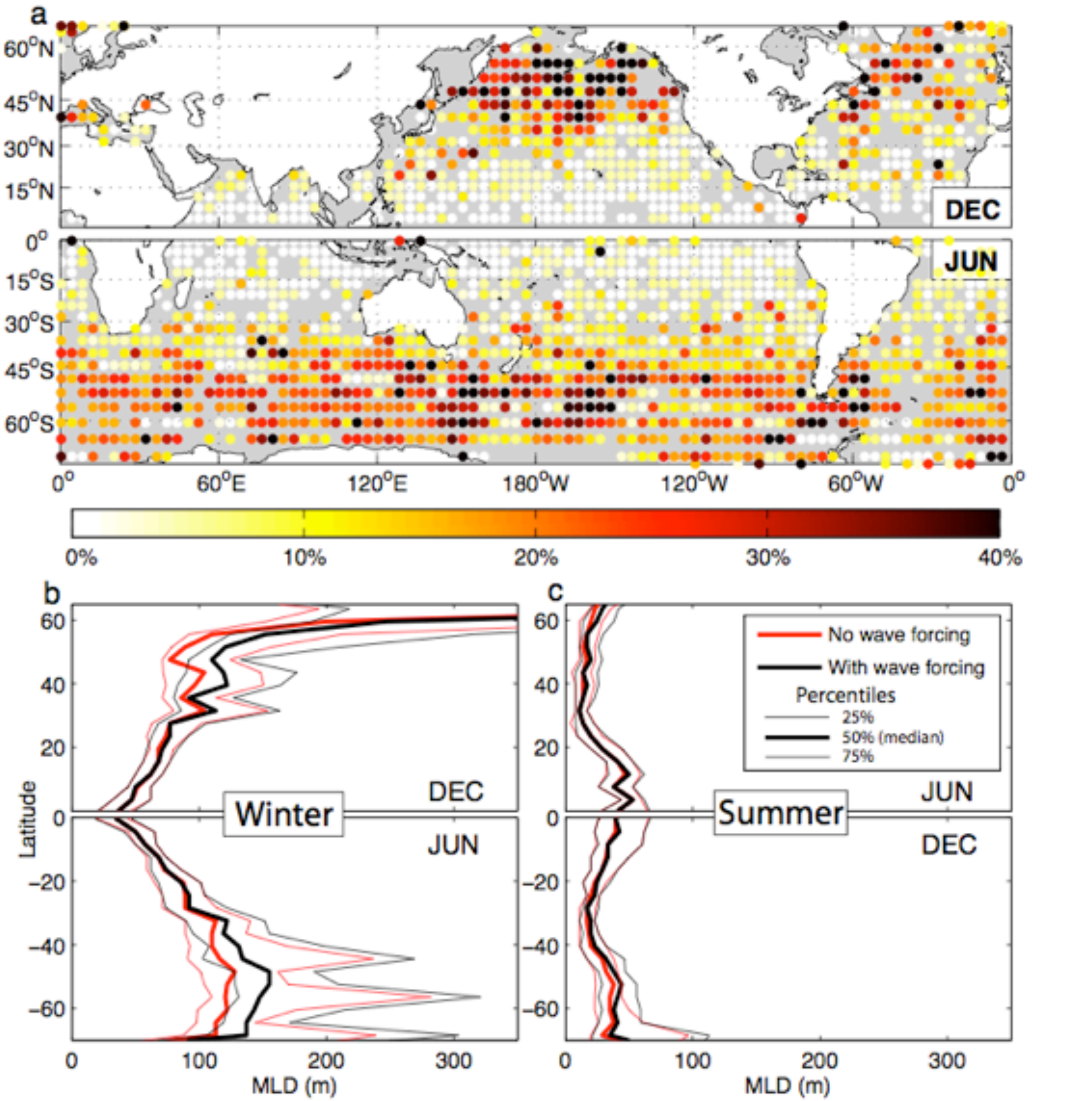

Figure 3. Contribution of Langmuir turbulence to global mixed layer depth. a) Percentage increase in mixed-layer depth with wave forcing relative to no wave forcing when Langmuir turbulence is parameterized [*Harcourt*, 2013] into a 1-d mixed layer model (SM 7) 180 days after a near-summer solstice initial profile; b) Zonal median (thick line) mixed layer depth and 25th and 75th percentiles, thin lines) 180 days after near-summer solstice initial profile with (black) and without (red) wave forcing; c) As for b) 365 days after initial profile.

E. A. D'Asaro, J. Thomson, A. Y. Shcherbina, R. R. Harcourt, M. F. Cronin, M. A. Hemer, and B. Fox-Kemper. Quantifying upper ocean turbulence driven by surface waves. Geophysical Research Letters, 2013. in press.

Waves in Climate Models

- Adding wave models into climate models is now done at NCAR, GFDL, CSIRO, FIO, ECMWF/Hadley
- Substantial mixed layer deepening is seen from Langmuir turbulence, especially in S. Ocean.
- Need to:
  - Cross-check extant parameterizations
  - Cross-check different models
  - Retune other parameterizations (e.g., submeso restratification limiters).
  - Build "data waves" cheap & accurate version.
  - Explore other wave-driven processes (air-sea, bubbles, etc.)

The Character of the Mesoscale

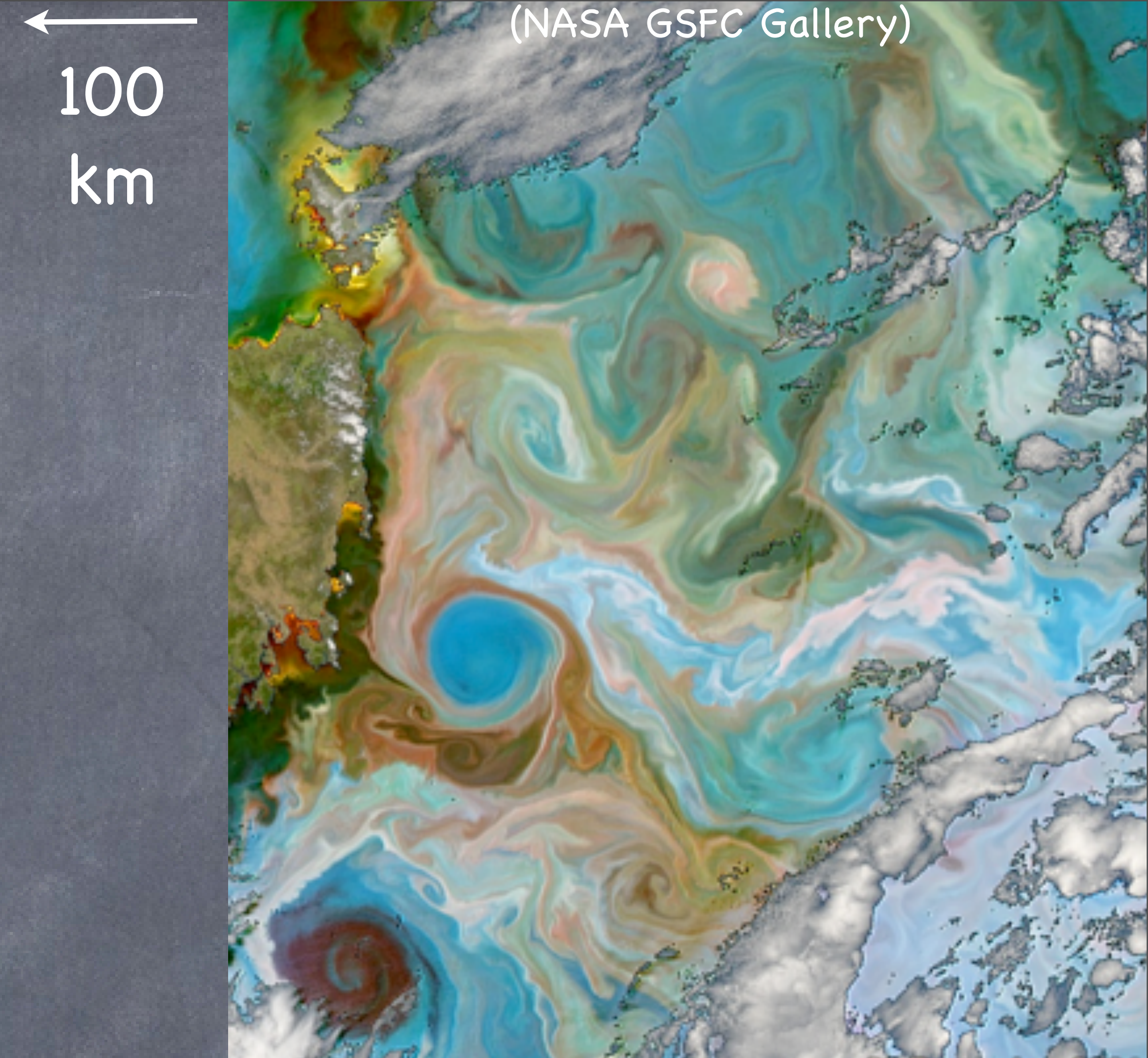

(Capet et al., 2008)

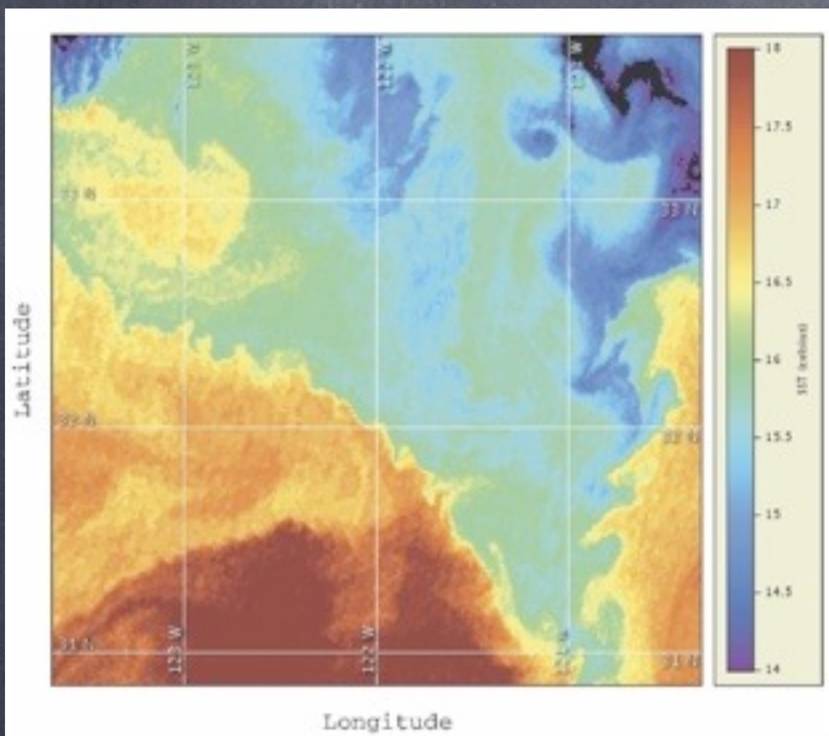

FIG. 16. Sea surface temperature measured at 1832 UTC 3 Jun 2006 off Point Conception in the California Current from CoastWatch (http://coastwatch.pfeg.noaa.gov). The fronts between recently upwelled water (i.e., 15°–16°C) and offshore water (≥17°C) show submesoscale instabilities with wavelengths around 30 km (right front) or 15 km (left front). Images for 1 day earlier and 4 days later show persistence of the instability events.

- Boundary Currents
- Eddies
- Ro=O(0.1)
- Ri=O(1000)
- Full Depth
- Eddies strain to produce Fronts
- 100km, months

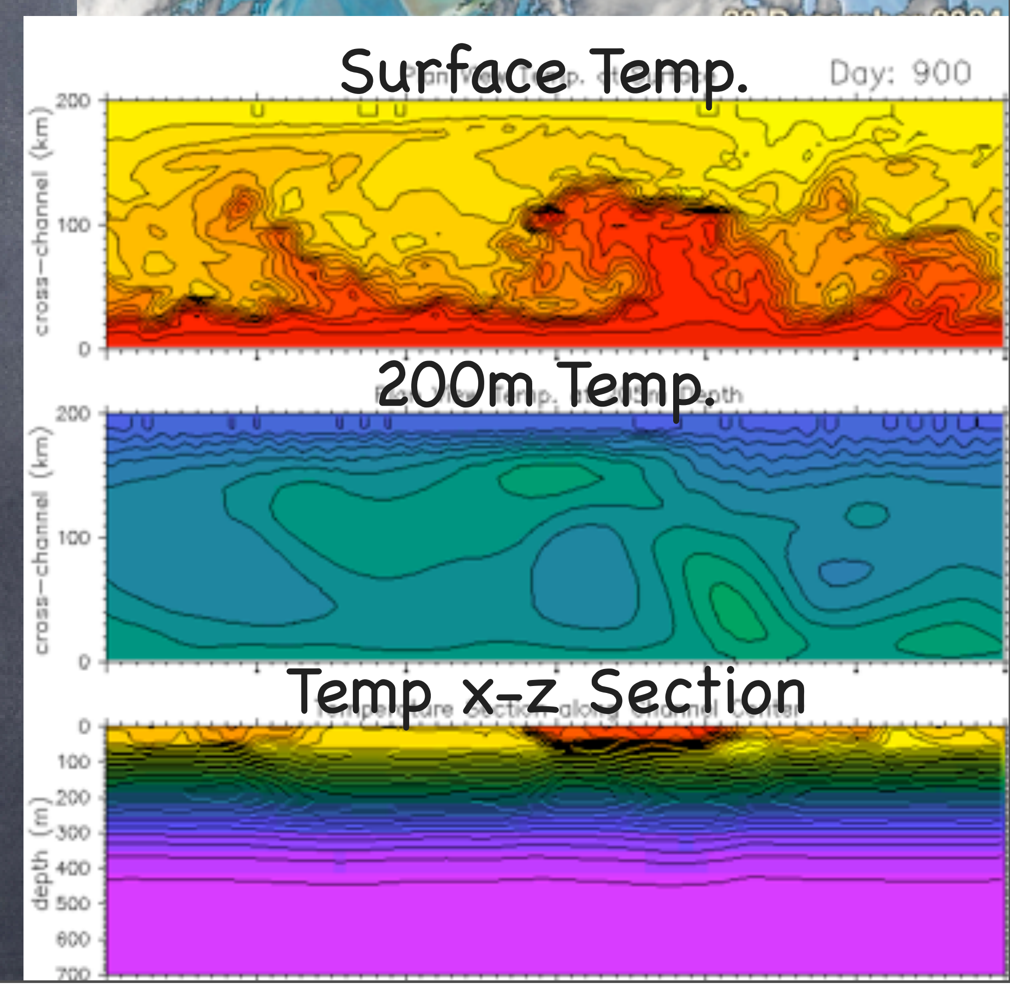

Eddy processes mainly baroclinic & barotropic instability. Parameterizations of baroclinic instability (GM, Visbeck...).

Parameterization of Mesoscale Eddies Scott Reckinger (New Primary)

- Continuity and tracer evolution (Boussinesq with no irreversible effects)

$$\nabla \cdot \vec{u} = 0$$

$$\partial_t \phi + \nabla \cdot \vec{u}\phi = 0$$

- Reynolds averaged equations

$$\vec{u} = \langle \vec{u} \rangle + \vec{u}'$$
$$\phi = \langle \phi \rangle + \phi'$$

$$\langle \vec{u}' \rangle = \vec{0}$$
$$\langle \phi' \rangle = 0$$

$$\nabla \cdot \langle \vec{u} \rangle = 0$$

$$\partial_t \langle \phi \rangle + \langle \vec{u} \rangle \cdot \nabla \langle \phi \rangle = -\nabla \cdot \langle \vec{u}' \phi' \rangle$$

Needs closure!

- Tracer eddy flux modeled as

$$\langle \vec{u}' \phi' \rangle = -\bar{\bar{J}} \cdot \nabla \langle \phi \rangle$$

Parameterization of Mesoscale Eddies

- Split tensor into symmetric and antisymmetric parts

$$\bar{\bar{J}} = \bar{\bar{K}} + \bar{\bar{A}}$$

mixing
dissipative
symmetric
eddy diffusivity tensor
reduce global tracer variance

stirring
advective
antisymmetric
eddy transport tensor
zero tracer variance effect

- Governing tracer equation (drop average notation)

$$\partial_t \phi + \vec{u} \cdot \nabla \phi = \nabla \cdot \left(\bar{\bar{K}} + \bar{\bar{A}} \right) \cdot \nabla \phi$$

Traditional Gent-McWilliams

$$S_x = -\frac{\partial_x \rho}{\partial_z \rho}$$
$$S_y = -\frac{\partial_y \rho}{\partial_z \rho}$$
$$S^2 = S_x^2 + S_y^2$$

- Align harmonic (horizontally isotropic) diffusion of tracers along neutral (isopycnal) surfaces with **diffusive flux is down the tracer gradient**

$$\bar{\bar{K}} = \begin{pmatrix} 1 & 0 & S_x \\ 0 & 1 & S_y \\ S_x & S_y & S^2 \end{pmatrix} \kappa$$

$$\vec{F}_K = -\bar{\bar{K}} \cdot \nabla \phi$$

- Eddy-induced stirring flattens neutral slopes and releases stored potential energy with **skew flux is perpendicular to the tracer gradient**

$$\bar{\bar{A}} = \begin{pmatrix} 0 & 0 & -S_x \\ 0 & 0 & -S_y \\ S_x & S_y & 0 \end{pmatrix} \kappa$$

$$\vec{F}_A = -\bar{\bar{A}} \cdot \nabla \phi$$

Anisotropic

$$S_x = -\frac{\partial_x \rho}{\partial_z \rho}$$
$$S_y = -\frac{\partial_y \rho}{\partial_z \rho}$$
$$S^2 = S_x^2 + S_y^2$$
$$\vec{S} = (S_x, S_y)$$

- Generalize to anisotropic horizontal diffusion
  - Symmetric diffusivity tensor
    - real eigenvalues => diffusivity values
    - orthogonal eigenvectors => principal axes
  - When the tracer gradient is partly orientated along a principal axis, the amount of diffusion in that direction is given by the associated eigenvalue and the tracer gradient projection

$$\bar{\bar{K}}_H = \begin{pmatrix} K_{xx} & K_{xy} \\ K_{xy} & K_{yy} \end{pmatrix} \qquad \bar{\bar{K}} = \left(\begin{array}{c|c} \bar{\bar{K}}_H & \bar{\bar{K}}_H \cdot \vec{S} \\ \hline \vec{S} \cdot \bar{\bar{K}}_H & \vec{S} \cdot \bar{\bar{K}}_H \cdot \vec{S} \end{array}\right)$$

Anisotropic

$$S_x = -\frac{\partial_x \rho}{\partial_z \rho}$$
$$S_y = -\frac{\partial_y \rho}{\partial_z \rho}$$
$$S^2 = S_x^2 + S_y^2$$
$$\vec{S} = (S_x, S_y)$$

- The advective stirring has been historically associated with an eddy-induced bolus velocity and streamfunction

$$\vec{u}^* = \nabla \times \vec{\psi} = -\nabla \cdot \bar{\bar{A}}$$

$$\bar{\bar{A}} = \left(\begin{array}{cc:c} 0 & 0 & \\ 0 & 0 & -\bar{\bar{K}}_H \cdot \vec{S} \\ \hdashline \multicolumn{2}{c:}{\vec{S} \cdot \bar{\bar{K}}_H} & 0 \end{array}\right) = \begin{pmatrix} 0 & \cancel{\psi_3} & -\psi_2 \\ -\cancel{\psi_3} & 0 & \psi_1 \\ \psi_2 & -\psi_1 & 0 \end{pmatrix}$$

- In the anisotropic case, the streamfunction components involve both isopycnal slope directions
- The streamfunction is used to formalize the Near Surface Eddy Flux Parameterization (NSEF)

Eddy Transport Operator

- Associate a functional, where the functional derivative is equal to the diffusive operator
    - Avoid introducing $2\Delta x$ computational modes that can lead to numerical stability issues
    - Ensure consistency by reducing global variance

$$\mathcal{G}(\phi) = -\frac{1}{2}\int dV \nabla\phi \cdot \bar{\bar{K}} \cdot \nabla\phi$$

$$\frac{\delta\mathcal{G}(\phi)}{\delta\phi} = R(\phi) \equiv \nabla \cdot \bar{\bar{K}} \cdot \nabla\phi$$

Griffies et al. (98), Smith & Gent (02)

Discretization of the Eddy Transport Operator

- **Discrete functional** is the **global sum** of the discrete integrand
- **Discrete diffusion operator** at a point is the discrete functional derivative with respect to ϕ_{ijk}
  - Requires a **local sum** of only the cells whose contribution to $\mathcal{G}(\phi)$ depends on ϕ_{ijk}
- Split cell into 8 subcells + 24 neighboring subcells

$$\mathcal{G}(\phi) = \frac{1}{2} \sum_{ijk} \sum_{n=1}^{8} v_{ijkn} \left[K_{xx} \left(\partial_x \phi + S_x \partial_z \phi \right)^2 + K_{yy} \left(\partial_y \phi + S_y \partial_z \phi \right)^2 + 2K_{xy} \left(\partial_x \phi + S_x \partial_z \phi \right) \left(\partial_y \phi + S_y \partial_z \phi \right) \right]$$

$$R_{ijk} = -\frac{1}{V_{ijk}} \frac{\partial \mathcal{G}(\phi)}{\partial \phi_{ijk}}$$

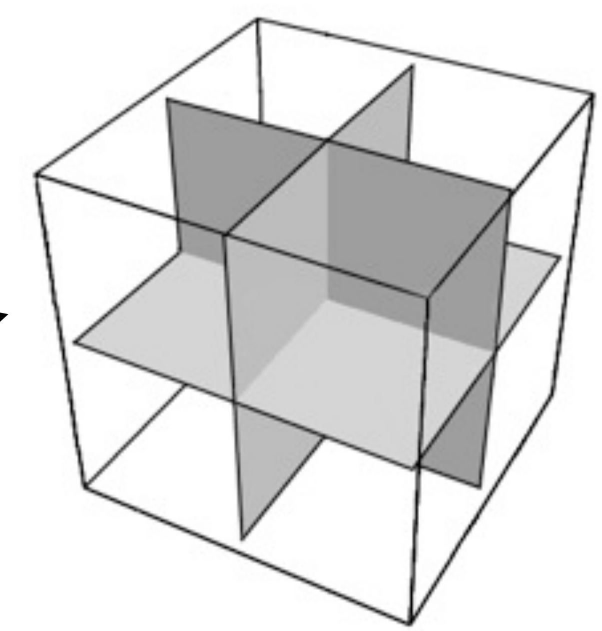

Discretization of the Eddy Transport Operator

- Advective tensor terms discretized in the same way as the contributions to $\mathcal{G}(\phi)$ from the off-diagonal elements of the discretized diffusivity tensor

$$R(\phi) + B(\phi) \equiv \nabla \cdot \left(\bar{\bar{K}} + \bar{\bar{A}} \right) \cdot \nabla \phi$$

$$\bar{\bar{K}} = \begin{pmatrix} \bar{\bar{K}}_H & \bar{\bar{K}}_H \cdot \vec{S} \\ \vec{S} \cdot \bar{\bar{K}}_H & \vec{S} \cdot \bar{\bar{K}}_H \cdot \vec{S} \end{pmatrix}$$

$$\bar{\bar{A}} = \begin{pmatrix} 0 & 0 & \\ 0 & 0 & -\bar{\bar{K}}_H \cdot \vec{S} \\ \vec{S} \cdot \bar{\bar{K}}_H & & 0 \end{pmatrix}$$

$$S_x = -\frac{\partial_x \rho}{\partial_z \rho}$$

$$S_y = -\frac{\partial_y \rho}{\partial_z \rho}$$

$$S^2 = S_x^2 + S_y^2$$

$$\vec{S} = (S_x, S_y)$$

Discretization of the Anisotropic Operator

- Requires true 3D volume integration
  - Terms with derivatives in all 3 dimensions e.g. $\partial_z \left[K_{xy} S_y \partial_x \phi\right]$ or $2\partial_z \left[K_{xy} S_x S_y \partial_z \phi\right]$
- Sensitive to rapid changes of the grid spacing lengths among neighboring cells
  - Accurate subcell volume calculations
  - Appropriate grid spacing lengths for discrete differentiation
- NSEF parameterization - streamfunction and the associated horizontal diffusion has modifications for the anisotropic case

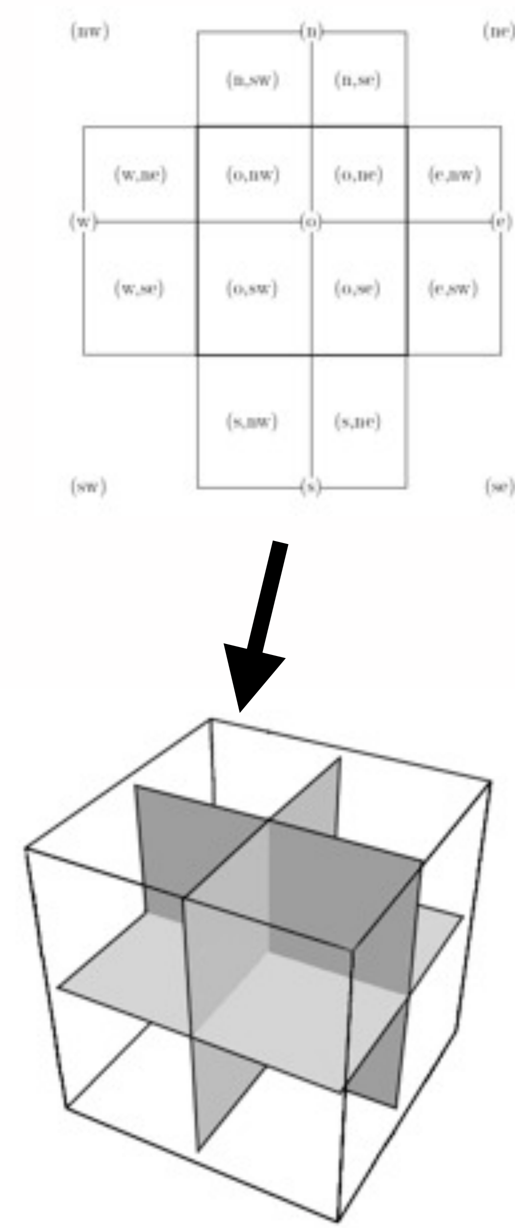

Ongoing/Future Work

- Advance the work of Smith and Gent (2004) - North Atlantic simulations using anisotropic GM
- Global simulations using Large and Yeager (2009) dataset - to show the effectiveness of including anisotropy
- Model enhancements, such as allowing partial bottom cells

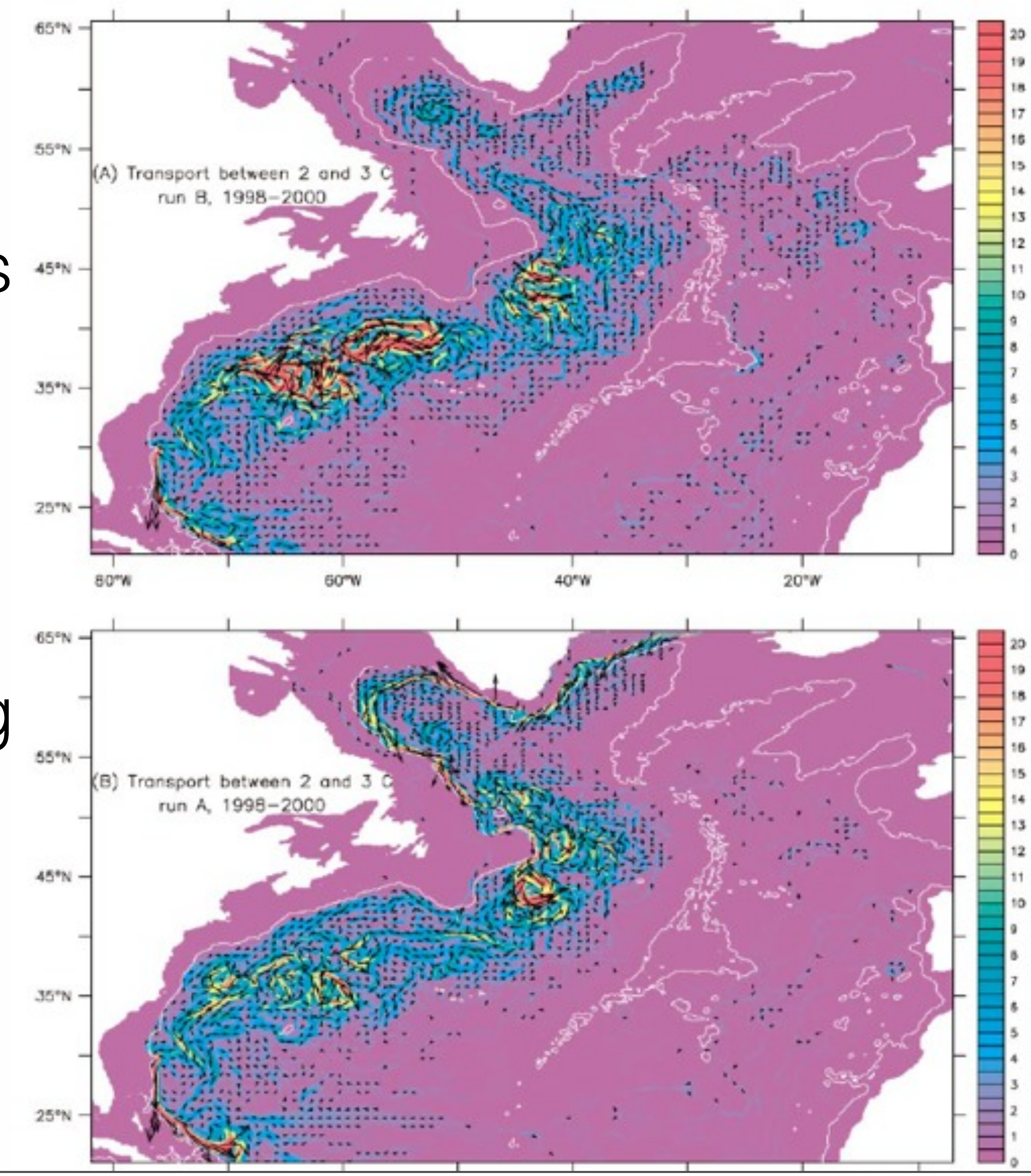

One eigenvalue is similar to either N^2 param (Danabasoglu & Marshall) or Eden & Greatbatch

Other is larger, probably due to shear dispersion

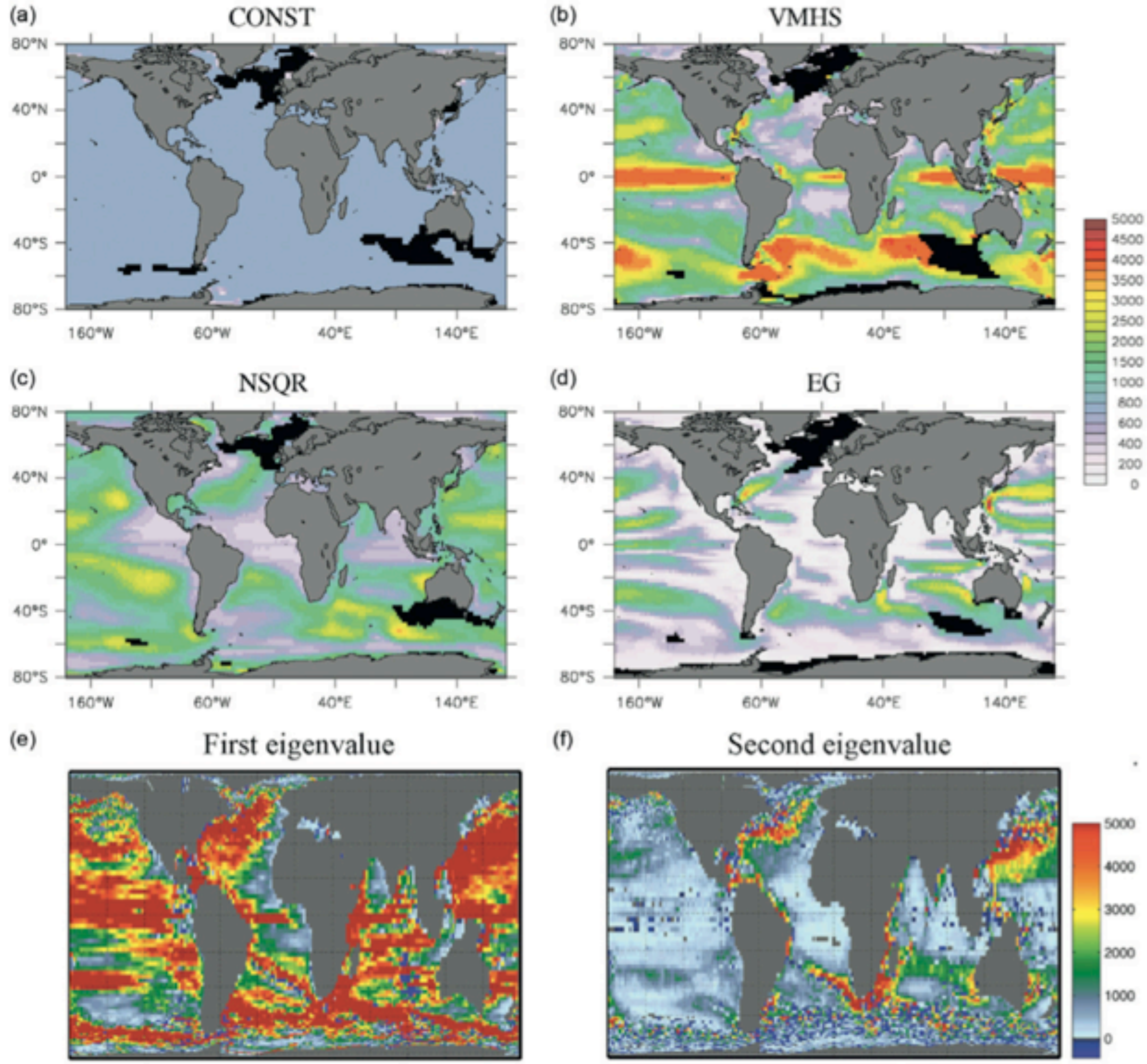

FIGURE 8.6 Comparison of diffusivity variations realized using different common parameterizations of spatial variation of (isotropic) diffusivity $K_{\alpha\beta}=\kappa$. (a) Constant diffusivity, (b) Visbeck et al. (1997), (c) Danabasoglu and Marshall (2007), (d) Eden and Greatbatch (2008), and (e and f) first and second eigenvalue from Figure 8.5. Black areas result from landmarks on the sphere remapping onto this projection. *Figures (a–d) are taken from Eden et al. (2009).*

B. Fox-Kemper, R. Lumpkin, and F. O. Bryan. Lateral transport in the ocean interior. In G. Siedler, S. M. Griffies, J. Gould, and J. A. Church, editors, Ocean Circulation and Climate: A 21st century perspective, volume 103 of International Geophysics Series, chapter 8, pages 185-209. Academic Press (Elsevier Online), 2013.

Conclusions & Status
Scott Reckinger (new)

- Anisotropic GM/Redi is now coded in CESM/POP
- Compiles & runs stably in ocean-only mode. Includes extension of transition layer physics to anisotropic K.
- Need to:
  - Cross-check vs. old GM/Redi code for backwards compatibility
  - Run control cases in coupled & Ocean-Only modes
  - Run simple aniso cases--By OS14
  - Implement physics params leading to anisotropic transports: shear dispersion, PV barriers
  - Implement & cross-check in different models